RESEARCH HIGHLIGHT

Surface Instabilities and Dislocation Patterns

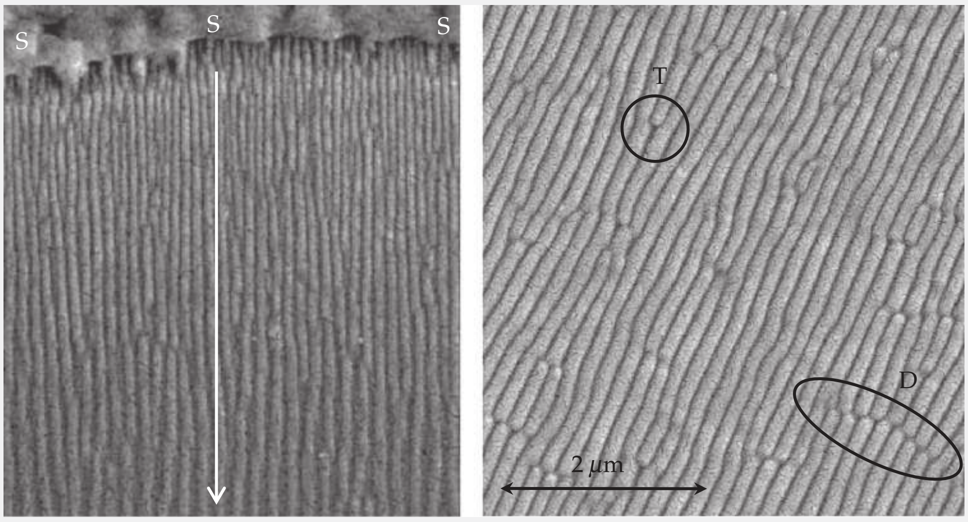

1.0. Ripples on the (110) surface of yttria-stabilized zirconia formed by diffusional doping.

(*a*) Scanning electron microscope image showing solid sources (S) of a rare-earth oxide that diffuses in the direction of the arrow. The ripples mound up by surface diffusion, in order to relieve coherency stresses caused by the misfitting dopant. The competition between strain energy and surface energy gives rise to the Asaro-Tiller-Grinfeld instability. Under a surface-diffusion mechanism, the characteristic wavelength of the pattern varies inversely with the square of the stress. The wavelength increases with increasing distance from the diffusion source (decreasing stress). (*b*) Defects in the self-assembled pattern include single terminations (T) and disregistries (D) that arise when separately initiated packets impinge on one another. The single terminations resemble edge dislocations, whereas the disregistries between packets resemble stacking faults. The refinement of the pattern (*a*) is achieved by the effective climb of terminations.

Contributed by H. M. Ansari, The Ohio State University (USA) (Ansari 2015). Panel (*a*) image courtesy of H. M. Ansari. Panel (*b*) image reprinted (with annotations) from Ansari (2012) by permission of the author.

© in this web service Cambridge University Press

CAMBRIDGE

Cambridge University Press
978-0-521-86436-7 — Theory of Dislocations
Peter M. Anderson , John P. Hirth , Jens Lothe
Excerpt
More Information

1. Introductory Material

1.0 KEY DEVELOPMENTS

- Axioms, Principles, and Theorems
  - Axiom 1.1: sign reversal of **b** and **ξ** — p. 13
  - Axiom 1.2: sum of **b** at a node — p. 16
  - Axiom 1.3: dislocation motion and relative slip — p. 17
  - continuity of dislocations, principle — p. 14, Eq. 1.10
  - equivalent Burgers circuits, principle — p. 15
- Definitions
  - Burgers circuit — p. 11
  - Burgers vector **b** — p. 12
  - climb — p. 10
  - components, edge vs. screw — Eqs. 1.6, 1.7
  - conservative motion — p. 10
  - cross slip — p. 17
  - curvature κ_{ij} — p. 18
  - disclinations — p. 5
  - dislocation density ρ — Eq. 1.9
  - dislocation density tensor $\boldsymbol{\alpha}$, Nye — Eq. 1.9
  - dislocation symbol ⊥ — p. 11
  - edge dislocation — p. 7, 9
  - Frankel sinusoidal stress — Eq. 1.1
  - glide, glide plane — p. 10, 16
  - Hooke's law — Eq. 1.2
  - Kronecker delta function δ_{ij} — Eq. 1.11
  - mixed dislocation — p. 15
  - node, dislocation — p. 15
  - nonconservative motion — p. 10
  - prismatic loop — p. 8
  - screw dislocation — p. 7, 9
    - right-handed — p. 14
    - left-handed — p. 14
  - sense **ξ** — p. 11
  - slip — p. 10
  - traces — Figure 1.29
  - Volterra dislocations — p. 4

© in this web service Cambridge University Press www.cambridge.org

CAMBRIDGE

Cambridge University Press
978-0-521-86436-7 — Theory of Dislocations
Peter M. Anderson , John P. Hirth , Jens Lothe
Excerpt
More Information

1.1 INTRODUCTION

In this chapter, the historical development of the concept of a dislocation and some elementary conventions to describe dislocations and their properties are presented. The physical phenomena that led to the discovery of dislocations and the early mathematical work for dislocation theory are also discussed. Today, many types of observations provide direct evidence of dislocations in crystals; selected examples are presented. The formal geometric properties of dislocations comprise the latter portion of the chapter. Some simple axioms result, forming the basis of tensorial and continuum descriptions of dislocations.

1.2 PHYSICAL BASIS FOR DISLOCATIONS

1.2a Early Work

Definition: Volterra dislocations

The first suggestion of dislocations probably occurred in the nineteenth century, when studies (Mügge, 1883; Ewing and Rosenhain, 1899) revealed slip bands or slip packets within plastically deformed metals. Such features arose from relative shear within the specimen. This interpretation remained obscure initially. However, the discovery that metals are crystalline supported the concept that deformation could occur by relative slip across rational crystal planes.

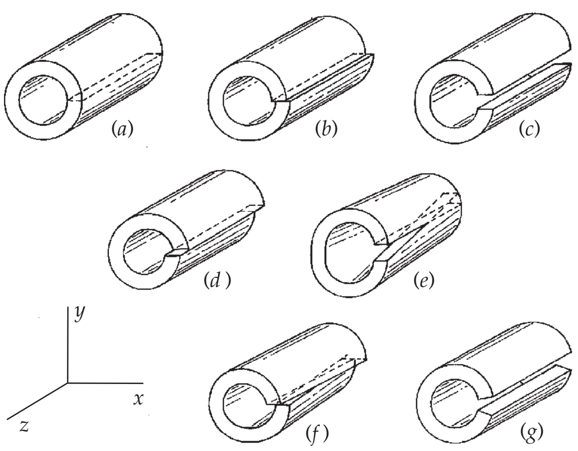

Figure 1.1. A cylinder (*a*) as originally cut, and (*b*) to (*g*), as deformed to produce the six types of dislocations as proposed by Volterra (1907).

Volterra (1907) and others, notably Love (1927), studied the elastic response of homogeneous isotropic media. These studies considered a cylinder that is cut along the z axis (Figure 1.1*a*) and subsequently deformed (Figures 1.1*b*–*g*). Some of these deformation operations correspond to uniform slip along the entire cut (e.g., Figures 1.1*b*, *d*) and some of the resulting configurations correspond to dislocations. However, this work was not connected to crystalline slip until the late 1930s, after dislocations had been postulated as crystalline defects. Configurations (*b*) and (*c*) in Figure 1.1 correspond to edge dislocations as the relative slip

© in this web service Cambridge University Press www.cambridge.org

Cambridge University Press
978-0-521-86436-7 — Theory of Dislocations
Peter M. Anderson , John P. Hirth , Jens Lothe
Excerpt
More Information

or opening is uniform within the cut and also perpendicular to the cylinder axis. Configuration (*d*) corresponds to a screw dislocation since the relative slip is uniform and parallel to the axis. Configurations (*e*), (*f*), and (*g*) have a nonuniform relative slip or opening across the cut and correspond to *disclinations* (Harris 1974). The displacements from an isolated disclination are proportional to the outer cylinder radius and hence they generate long-range stress. However, disclination dipoles do not generate long-range stress, and they can be used to describe grain boundaries by placing them at grain boundary junctions (Chapter 19). Overall, isolated unit disclinations in metal crystals do not appear because of their large energy and therefore they are not discussed further.

Definition: Disclinations
• Figure 1.1*e*–*g*.

The discovery of x-rays and of x-ray diffraction established crystallinity in metals. Darwin (1914a,b) and Ewald (1917) subsequently observed that the intensity of reflected x-ray beams was about twenty times the expected value for a perfect crystal. The intensity in a perfect crystal is expected to be low due to the long absorption path provided by multiple internal reflections. Further, the observed width of reflected beams was about 1 to 30 minutes of arc – many times larger than the few seconds expected for a perfect crystal.

These discrepancies motivated a theory that real crystals consisted of roughly equiaxed crystallites that are small (10^{-4} to 10^{-5} cm in diameter) and slightly misoriented with respect to one another, with amorphous material at the intercrystalline boundaries. In this "mosaic-block" theory, the crystallite size limits the absorption path and accounts for the observed reduced intensity, whereas the misorientation accounts for the observed larger beam width. It was not appreciated then that the crystallite boundaries actually consist of arrays of dislocation lines.

The existence of dislocations is also implied by studies of crystal growth. Studies of nucleation by Volmer (1939) followed the ideas of Gibbs (1948) and suggested that nucleation of new layers during layer growth of perfect crystals required supersaturations of about 1.5. However, experiments showed that crystals grew under nearly equilibrium conditions; see, for example, the work of Volmer and Schultze (1931) on iodine. Frank (1949a,b) resolved this discrepancy by postulating that growth could proceed at lower supersaturations, by the propagation of ledges that are present where spiral dislocations intersect surfaces.

Several other early studies also support the existence of dislocations. For example, point defects in a crystal rapidly equilibrate upon a change in temperature. This suggests the presence of internal sources and sinks for point defects in crystals. Dislocations and arrays thereof can provide such sources and sinks.[1] Other examples are not discussed because they were developed at a later time or were less striking than the examples cited. However, a final example involving the strength of a perfect crystal is treated in detail in Section 1.2b. It stimulated early work on dislocations and it employs a phenomenological approach that can be applied to many other dislocation problems.

1.2b Theoretical Shear Strength of a Perfect Crystal

The realization that metals are crystalline spawned studies to determine the strength of perfect crystals. The classical work by Frenkel (1926) involves an idealized shear stress versus relative shear displacement relation, shown in Figure 1.2. A crystal shearing on a rational plane is assumed to have an energy $W(x)$ per unit area of plane that fluctuates periodically with the relative shear translation x. The period

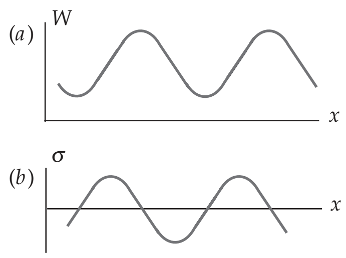

1.2. (*a*) A periodic lattice potential W as a function of the relative shear translation x and (*b*) the corresponding plot of shear stress σ vs. x.

[1] Seidman and Balluffi (1965) have shown that dislocations act as vacancy sources in up-quenched gold.

© in this web service Cambridge University Press www.cambridge.org

CAMBRIDGE

Cambridge University Press
978-0-521-86436-7 — Theory of Dislocations
Peter M. Anderson , John P. Hirth , Jens Lothe
Excerpt
More Information

equals b, the magnitude of a simple lattice-translation vector. The contribution of surface steps created where the shear plane intersects a free surface is neglected.

The applied shear stress required to accomplish a relative shear translation scales as $\sigma \sim dW/dx$. Frenkel approximated the periodic energy by a simple trigonometric function; e.g., $W(x) = [1 - \cos(2\pi x/b)]$. When differentiated, this yields

Definition: Frenkel sinusoidal stress
• Figure 1.2

$$\sigma = \sigma_{\text{theor}} \sin \frac{2\pi x}{b} \tag{1.1}$$

where σ_{theor} is the theoretical shear strength of the crystal. If the shear translation x <<d, the interplanar spacing, then Eq. (1.1) takes the form $\sigma = 2\pi x \sigma_{\text{theor}}/d$ This result can be compared to the shear counterpart to Hooke's law,

Definition: Hooke's Law

$$\sigma = \mu \frac{x}{d}, \quad \frac{x}{d} << 1 \tag{1.2}$$

where μ is the elastic shear modulus. The comparison reveals that

Theoretical shear strength
• Estimate based on Frankel sinusoidal stress

$$\sigma_{\text{theor}} = \frac{\mu}{2\pi}\frac{b}{d} \quad \left(\approx \frac{\mu}{5} \text{ if } b \approx d\right) \tag{1.3}$$

The predicted theoretical strength of Eq. (1.3) is ~ 0.2μ. This is orders of magnitude larger than experimental values of the maximum resolved shear stress to initiate plastic flow in metals. Such measurements were $(10^{-3}$ to $10^{-4})\mu$ at the time of Frenkel's work but they have decreased further with the advent of more sophisticated test equipment.

Equation (1.3) probably overestimates σ_{theor} because various semiempirical interatomic force laws predict a more rapid decrease in attractive forces with interatomic spacing than suggested by the sinusoidal form in Figure 1.2. Further, additional minima may exist in the W–x plot, corresponding to twin or other special orientations. Mackenzie (1949) found that σ_{theor} could be reduced to $\mu/30$ when central forces for close-packed lattices are used. However, this approach may underestimate σ_{theor} because it neglects small directional forces present in such lattices. Also, the contribution of thermal stresses, treated in detail later, reduce σ_{theor} to less than $\mu/30$ only near the melting point. At room temperature, all theoretical estimates tend to fall within $\mu/15 > \sigma_{\text{theor}} > \mu/30$ (Kelly 1973; Ogata et al. 2009). These estimates agree well with the maximum values (~ $\mu/15$) of resolved shear stress to initiate plastic flow in (presumably perfect) whiskers of various metals (Brenner 1958).

Theoretical shear strength
• Other estimates

Whiskers are the exception, however. Experimental work on bulk copper (Tinder and Washburn 1964) and zinc (Tinder 1964) indicates that plastic deformation begins at stresses ~ $10^{-9}\mu$. Thus, except for whiskers, the discrepancy between σ_{theor} and experimental values is even larger than was first supposed.

Stress for plastic deformation
• Experimental measurements

EXERCISE 1.1. Carry out a calculation analogous to that of Frenkel but use a Morse function

$$W = W_0\left(e^{-2a(r-r_0)} - 2e^{-a(r-r_0)}\right) \tag{1.4}$$

for the interatomic potential, where W_0 and a are parameters and r_0 is the equilibrium separation of atoms. Such functions give good fits to P–V data, compressibility, and elastic constants in fcc crystals (Girifalco and Weizer (1959; 1960)). Show that $\sigma_{\text{theor}} = \mu b/20d$ when Eq. (1.4) is used instead of Eq. (1.1), and when $r_0 \sim b$,

© in this web service Cambridge University Press www.cambridge.org

CAMBRIDGE
Cambridge University Press
978-0-521-86436-7 — Theory of Dislocations
Peter M. Anderson , John P. Hirth , Jens Lothe
Excerpt
More Information

$x \sim r - r_0$, and the typical value $a = r_0$ are used. Also show that the maximum stress occurs at $x = 0.138b$ versus $x = 0.25b$ for the case in Figure 1.2. The similar outcomes suggest that the Frenkel model provides a reasonable order of magnitude estimate of σ_{theor}.

Subsequent to Frenkel's work, Masing and Polanyi (1923), Prandtl (1928), and Dehlinger (1929) proposed various defects that were precursors to the dislocation. For example, Figure 1.3 shows that sliding across weakly bonded planes creates defects. The sliding creates numerous sites where planes of atoms (lines in the 2D figure) terminate at slipped planes. These sites may be regarded as fractional dislocations. Yamaguchi (1929) came very close to the concept of an edge dislocation but viewed the effect of defects on deformation and hardening as being connected to lattice curvature. In 1934, Orowan (1934a,b), Polanyi (1934), and Taylor (1934) rationalized the aforementioned discrepancy between σ_{theor} and experimental measurements of yield strength by proposing the *edge* dislocation, depicted in Figure 1.4. It is signified by a line along the z axis, at which a half-plane of atoms is terminated in an otherwise perfect crystal. This line separates slipped and unslipped portions of a plane, where the relative slip is *perpendicular* to the line. Burgers (1939a,b) advanced the description of the *screw* dislocation, depicted in Figure 1.5. It is also signified by a line along the z direction that separates slipped and unslipped portions of a plane; however, the relative slip is *parallel* to the line.

Definition: Edge dislocation
• Figure 1.4

Interestingly, configurations such as Fig. 1.3 exist for liquid crystals.

Definition: Screw dislocation
• Figure 1.5

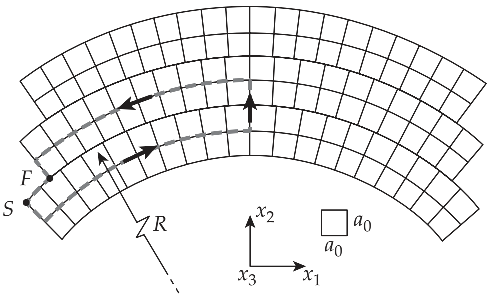

1.3. Imperfections in a crystal deformed by bending, according to Masing and Polanyi (1923). A Burgers circuit is superposed.

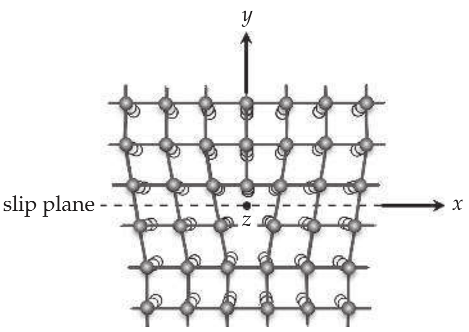

1.4. An edge dislocation in a simple cubic crystal.

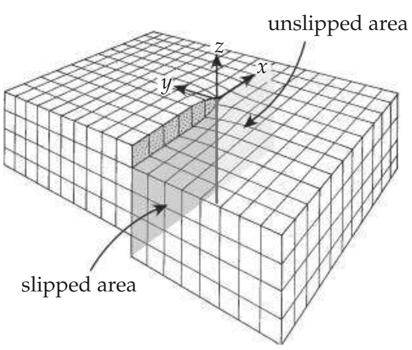

1.5. A screw dislocation in a simple cubic crystal.

1.2c Observations of Dislocations

Since 1950, an overwhelming number of observations have provided unequivocal evidence that dislocations exist in crystals. A few examples are presented; however, the reviews listed at the end of this chapter provide more extensive surveys.

Figure 1.6 shows an edge dislocation in a 2D raft of bubbles created by Bragg and Nye (1947). The dislocation corresponds to the termination of a plane of atoms in an otherwise perfect crystal. Possibilities among the many choices for the plane are *AO* or *BO*, where atom *O* (indicated by the arrow) is in the center of the diagram. The dislocation could be formed by imposing the relative shear depicted

© in this web service Cambridge University Press www.cambridge.org

CAMBRIDGE

Cambridge University Press
978-0-521-86436-7 — Theory of Dislocations
Peter M. Anderson , John P. Hirth , Jens Lothe
Excerpt
More Information

Definition: Growth spiral
• n-nonatriacontane
• Figure 1.7

Dislocation in a bubble raft
• Figure 1.6

at point C across the plane CD or by imposing the relative shear depicted at point C' across the plane $C'D$. Figure 1.7 shows a growth spiral in n-nonatriacontane. The growth is centered on a dislocation with a screw component, similar to Figure 1.5. After completion of the growth, the dislocation slipped out of the crystal, leaving behind a curved slip trace indicated by the arrow. Figure 1.8 shows a similar spiral on a {100} face of silver. The spiral steps are revealed by decoration and phase contrast microscopy and are only one atomic layer high. These observations and other cases of spirals reported in the literature[2] confirm Frank's postulate (Frank 1949a,b) that ledges can lower the supersaturation required for crystal growth.

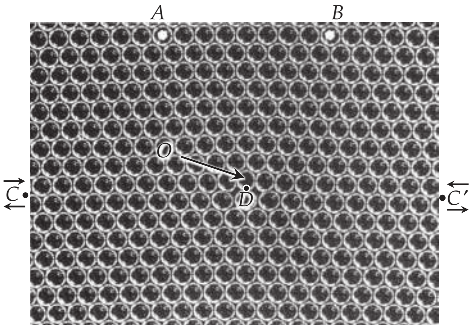

1.6. A 2D bubble raft with a dislocation at the bubble O in the center. From Bragg and Nye (1947). Reprinted (with minor annotations) by permission of the Royal Society.

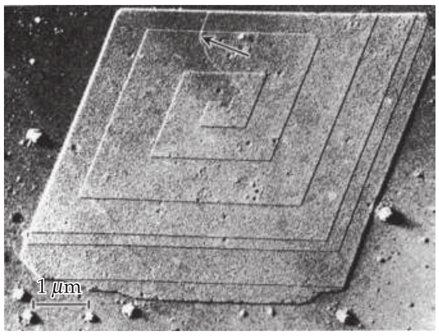

1.7. Growth spiral on an n-nonatriacontane crystal. The dislocation at the spiral center slipped out of the crystal following growth, leaving behind a slip trace. From Anderson and Dawson (1953). Reprinted by permission of the Royal Society.

Definition: Etch pits
• Figures 1.9, 1.11

Bond distortion near dislocations can enhance chemical etching where a dislocation emerges at a free surface and thus an *etch pit* can form. Similarly, this bond distortion can enable dislocations to serve as catalytic sites for precipitation from a solid solution. Dash (1957) formed etch pits at dislocations in silicon and decorated the dislocation lines with copper. The resulting observations by infrared transmission microscopy are in Figure 1.9. Figure 1.10 shows a silver halide sample with dislocations that are decorated by the precipitation of silver. The dislocations are *prismatic loops*, equivalent to areas within which a plane of atoms is missing or an extra layer of atoms exists. They can form near glass spheres (top of figure) during cooling, because of a difference in coefficient of thermal expansion between the spheres and matrix. Figure 1.11, from the extensive work of Gilman and Johnston (1957), is an example of etch pits at dislocation sites on {100} LiF surfaces.

Definition: Prismatic loops
• Figure 1.10

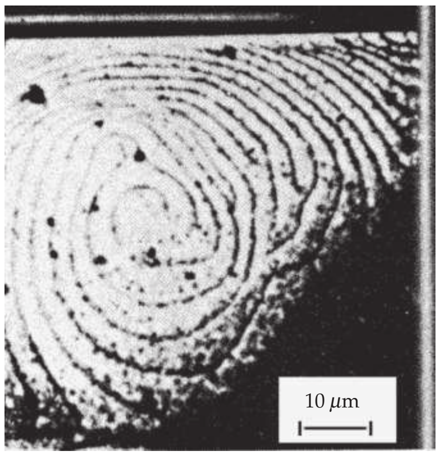

1.8. Decorated spiral-growth ledges on a silver crystal, indicating the presence of a dislocation at the spiral center during crystal growth. From Frank and Forty (1953). Reprinted by permission of the Royal Society.

Dislocations can be revealed by various optical techniques since radiation can be selectively diffracted in

[2] For example, Dumrul et al. (2002) shows atomic force microscope images of zeolite A, revealing pyramidal structures on {100} surfaces produced by growth spirals around screw dislocations.

© in this web service Cambridge University Press www.cambridge.org

CAMBRIDGE

Cambridge University Press
978-0-521-86436-7 — Theory of Dislocations
Peter M. Anderson , John P. Hirth , Jens Lothe
Excerpt
More Information

the highly distorted region near a dislocation. Figure 1.12 is a direct lattice image of a dislocation in a transmission electron micrograph. Figure 1.13 is a reflection x-ray micrograph revealing dislocations in lithium fluoride, while Figure 1.14 is a transmission x-ray micrograph showing dislocations in aluminum. Figure 1.15 is one of the earliest transmission electron micrographs from the extensive work of Hirsch et al. (1956, 1957, 1960) showing polygonized subboundaries (dislocation arrays) in aluminum. Figure 1.16 is a transmission micrograph showing dislocations in a Cu-7% Al alloy. Figure 1.17 is a transmission electron moiré pattern from Pashley (1957, 1958, 1965) showing dislocations in overlying Pd and Au {111} layers. Finally, Figure 1.18 is an ion emission pattern indicating dislocations in a platinum ion emission tip (Müller 1962). Other observations of dislocation are presented throughout the text.

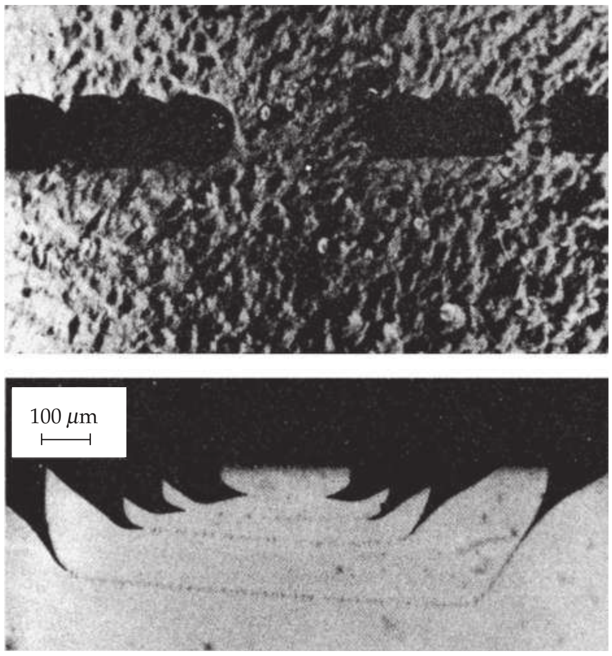

1.9. Chemical etch pits at copper-decorated dislocations in silicon, observed by infrared transmission microscopy. From Dash (1957). Reprinted by permission of the General Electric Company.

1.3 SOME ELEMENTARY GEOMETRIC PROPERTIES OF DISLOCATIONS

1.3a Displacement Associated with a Dislocation

Consider a perfect crystal cube sustaining a shear stress σ as shown in Figure 1.19*a*. The *edge dislocation* in Figure 1.19*b* is produced by a relative shear displacement b across the shaded portion of the internal plane. The dislocation is the internal line AA that separates the slipped and unslipped portions and terminates at the front and back surfaces with the symbol $\perp$. The nomenclature *edge* was coined to signify that the line AA terminates an inserted plane; that is, it is *perpendicular* to the relative displacement. Similarly, the relative displacement across the shaded plane in Figure 1.19*d* produces a *right-handed screw dislocation*, corresponding to the internal line AA that separates slipped and unslipped portions. The nomenclature *screw* denotes that the dislocation transforms the perfect crystal into a continuous spiral ramp; that is, the line AA is *parallel* to the relative slip. It is *right-handed* since a right-handed rotation about the surface normal $\mathbf{n}$ follows the helical surface and produces a displacement in the positive $\mathbf{n}$ direction. A left-handed screw is formed if the sign of the relative shear is reversed.

Definition: Edge dislocation
• Figure 1.19*b*

Definition: Screw dislocation
• Figure 1.19*d*

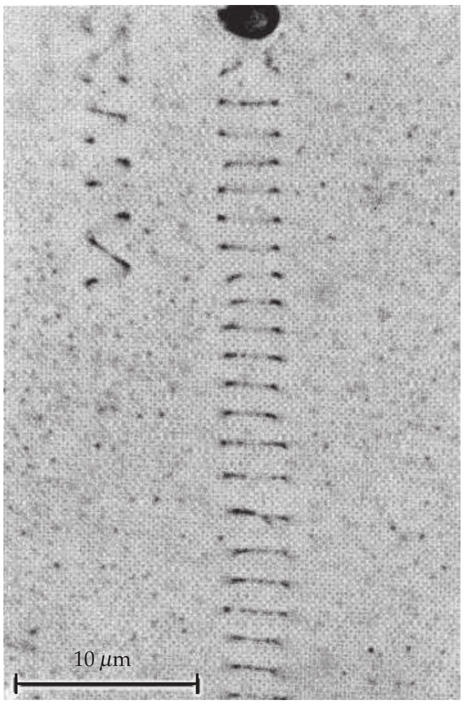

1.10. Dislocation loops in silver halide decorated by a precipitate of silver.

From Jones and Mitchell (1958). Image reprinted by permission of Taylor and Francis Ltd. www .tandfonline.com.

Motion of either the edge or screw dislocation in direction $\mathbf{v}$ in Figures 1.19*b*,*d* ultimately causes the dislocation to exit the crystal. Both cases produce complete shear of the

© in this web service Cambridge University Press www.cambridge.org

Cambridge University Press
978-0-521-86436-7 — Theory of Dislocations
Peter M. Anderson , John P. Hirth , Jens Lothe
Excerpt
More Information

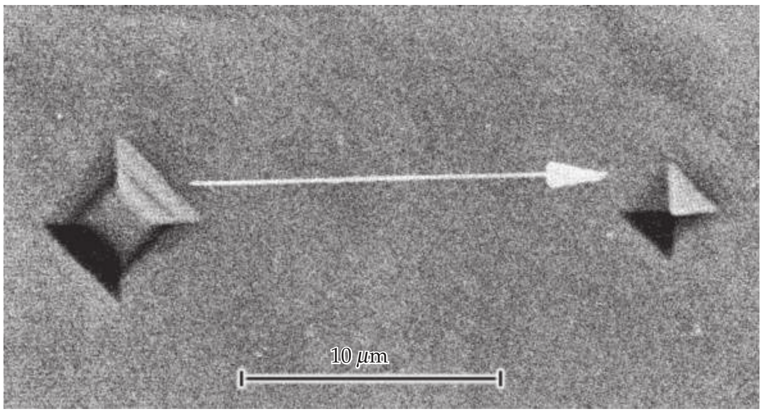

1.11. Dislocation motion as revealed by etch pits on a {100} surface of lithium fluoride. The original dislocation was etched, forming a pit on the left. The crystal was then deformed and reetched, producing a new, smaller pit on the right, at the new position of the dislocation. Fresh pits formed at the current site of a dislocation tend to have a sharp, pyramidal shape (right), whereas old pits at which the dislocation no longer resides tend to have a flat bottom after reetching (left). From Gilman and Johnston (1957). Reprinted by permission of the General Electric Company.

Definition: Conservative motion
• Figure 1.19*c*

Definitions: Glide Slip
• Figure 1.19*c*

cube as shown in Figure 1.19*c*. The resulting motion is *conservative*, meaning that the relative displacement lies within the slip plane, thereby conserving the total number of atoms and lattice sites. Conventionally, conservative motion of a single dislocation is called *glide* and that by several dislocations is called *slip*.

One can create the edge dislocation in Figure 1.19*f* by first making a cut and opening it up via an applied stress as shown in Figure 1.19*e*. An extra plane of material is then inserted to fill the cut, the applied stress is released, and the cut is closed up as to leave no gaps. The same process could be used to create the edge dislocation in Figure 1.19*b*, but the starting configuration would have a pre-existing ledge on the left face. For a single dislocation in a lattice, the added material corresponds to an extra *plane* of atoms. In this sense, the edge dislocations in Figures 1.19*b* and *f* could be created by introducing a dislocation near the top or bottom surfaces and then moving the dislocation vertically to the final center position. This type of dislocation motion is called *climb*. It is *nonconservative*, meaning the relative displacement produced by the dislocation motion does not lie within the plane of dislocation motion. Climb thus involves opening or closing of material. This is mitigated by the motion of interstitials or vacancies to or from the dislocation.

Definitions: Climb motion
Nonconservative motion

A general dislocation is represented by the symbol ⊥. For an edge dislocation, the

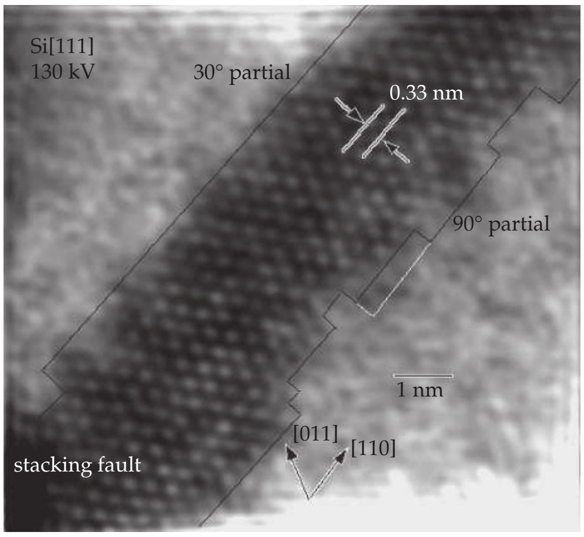

1.12. High resolution transmission electron micrograph of a thin film of silicon containing a stacking fault (diagonally oriented dark region), produced by dissociation of a 60° dislocation. This view along a [111] direction reveals that the stacking fault is parallel to (111) atomic planes, characterized by six-member rings. The black lines indicate a 30° partial dislocation along the upper boundary of the stacking fault and a 90° partial dislocation on the lower boundary. The steps or "kinks" along these lines are more frequent on the 90° partial. Kink motion can change the local position of a partial (e.g., the black vs. white line configuration of the 90° partial). Collective kink motion on both partials can move the stacking fault through the crystal. Image (with modifications) reprinted with permission from Kolar et al. (1996) by the American Physical Society, DOI: http://dx.doi.org/10.1103/PhysRevLett.77.4031.

© in this web service Cambridge University Press www.cambridge.org

CAMBRIDGE

Cambridge University Press
978-0-521-86436-7 — Theory of Dislocations
Peter M. Anderson , John P. Hirth , Jens Lothe
Excerpt
More Information

"leg" of the symbol points in the direction of the added material, as depicted in Figure 1.19*f*. The position of a screw dislocation is sometimes denoted by • rather than ⊥.

Definition: Dislocation symbol
• Figure 1.19*f*

1.3b The Burgers Vector

The relative displacement or *Burgers vector* **b** of a dislocation is defined by a procedure suggested by Frank (1951b). Considerable detail is provided because it is used in later chapters and inconsistencies exist in the literature.

Definition: Burgers vector
• Figure 1.20*b*

This formal definition holds for any elastic medium containing any distribution of dislocations and thus it can provide the net **b** for a collection of dislocations. However, it is usually applied to single or small numbers of dislocations.

Consider an edge dislocation in a simple cubic lattice as shown in Figure 1.20*a*. A section normal to a cube plane is shown so that the extra plane of atoms is situated in the upper half and terminates at point *O*. Figure 1.20*b* depicts a perfect reference lattice with lattice points specified by the translation vector m $\mathbf{t}_1 + n\,\mathbf{t}_2$, where m and n have integer values. The distortions in Figure 1.20*a* are large near the dislocation line at *O*. The distortions decrease with distance from *O*, although the two lattices might be displaced relative to one another.

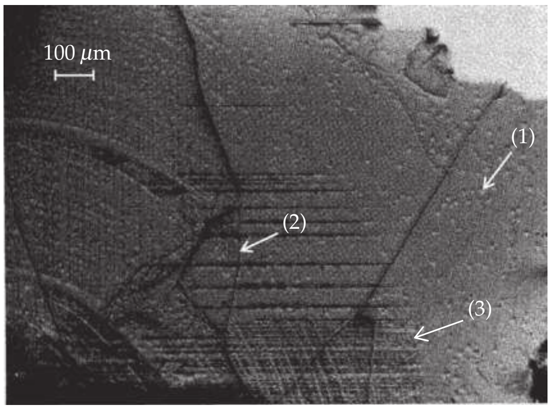

1.13. (220) Berg-Barrett x-ray-diffraction micrograph (Cr Kα) of an etched lithium fluoride crystal. Note (1) etch pits at dislocations, (2) subboundaries, and (3) dislocation lines. From Newkirk (1962). Reprinted with permission of the Minerals, Metals, and Materials Society.

A dislocation is specified by the Burgers vector **b** and the *sense* **ξ**, which is a unit vector parallel to the dislocation line. The direction of **ξ** can be chosen arbitrarily, *e.g.*, it may point into or out of the page in Figure 1.20*a*. **ξ** specifies the positive direction along the dislocation line and a closed loop or *Burgers circuit* is defined in a right-handed sense around **ξ**. The circuit must lie in "good" material where strain is small and displacements are well defined.

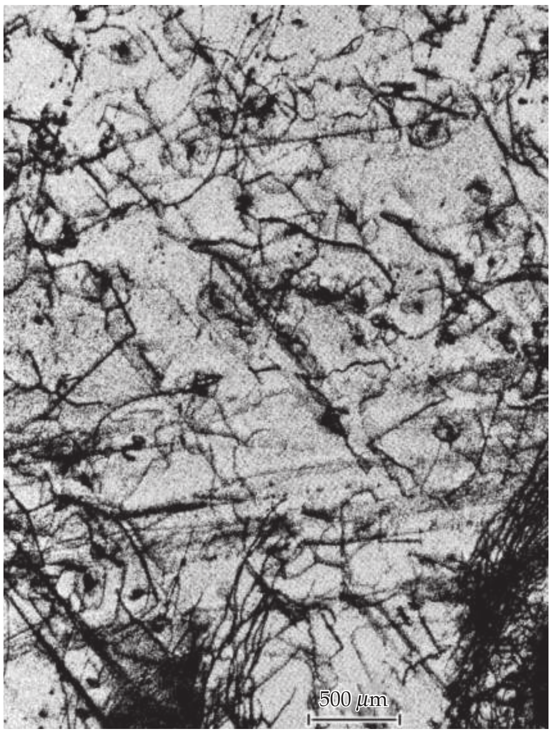

1.14. (220) Lang x-ray-transmission micrograph (Ag Kα) of a 1 mm thick aluminum single crystal with a very low density (~ 10^2/cm^2) of dislocation lines.

From Nøst (1965). Image reprinted (with minor modifications) by permission of Taylor & Francis Ltd, www.tandfonline.com.

Definition: Sense ξ
• Figure. 1.20

Definition: Burgers circuit
• Figure. 1.20

There are two conventions to define the Burgers vector **b**. The **FS**/*RH* convention (Bilby et al. 1955) uses a closed Burgers circuit in the crystal containing the dislocation. The circuit is drawn in a *right-handed* sense about **ξ**. In Figure 1.20*a*, **ξ** is chosen into the page and thus the Burgers circuit is clockwise, specified by *S-1-2-3-F*. The circuit would be counterclockwise if **ξ** were chosen out of the page. This same circuit of horizontal and vertical jumps

© in this web service Cambridge University Press www.cambridge.org